*Inorganic Materials, Vol. 40, No. 7, 2004, pp. 744–750. Translated from Neorganicheskie Materialy, Vol. 40, No. 7, 2004, pp. 853–859.*


# Structure and Properties of Nonstoichiometric $La_{1-x}Na_xMnO_{3\pm\gamma}$ Solid Solutions

**O. Z. Yanchevskii*, A. I. Tovstolytkin**, O. I. V'yunov*, D. A. Durilin*, and A. G. Belous***

** Vernadsky Institute of General and Inorganic Chemistry, National Academy of Sciences of Ukraine, pr. Akademika Palladina 32/34, Kiev, 03142 Ukraine*

*** Institute of Magnetism, National Academy of Sciences of Ukraine, pr. Vernadskogo 36b, Kiev, 03142 Ukraine*

*e-mail: yanch@ionc.kar.net*

Received August 1, 2003; in final form, December 9, 2003

**Abstract**—The structural, electrical, magnetic, and magnetoresistive properties of polycrystalline $La_{1-x}Na_xMnO_{3\pm\gamma}$ are studied in the range $0.08 \le x \le 0.16$. The solid solutions contain La and O vacancies and crystallize in the space group $R\bar{3}c$. The Curie temperature of the solid solutions depends not only on the formal charge state of Mn but also on the Na content, the amounts of La and O vacancies, and synthesis conditions. The synthesized materials are potentially attractive as room-temperature magnetic sensors.

## INTRODUCTION

The intimate relationship between the structural, electrical, and magnetic properties of lanthanum manganite ($LaMnO_3$) and related materials is a topic receiving much attention. Of particular interest is the colossal magnetoresistive response of doped manganites [1–3]. The presence of manganese ions in different oxidation states ($Mn^{3+}$ and $Mn^{4+}$) may result in a combination of ferromagnetism, metallic conduction, and a significant magnetoresistance: a decrease in electrical resistivity ρ in a magnetic field. The resistivity of such materials reaches a maximum near the ferromagnetic ordering temperature $T_C$. The temperature variation of magnetoresistance is similar to that of ρ: magnetoresistance also passes through a maximum near $T_C$. Above the Curie temperature, magnetoresistance is close to zero. Clearly, practical applications of the colossal magnetoresistive effect (magnetometers, magnetic sensors, ultrahigh-density magnetic recording media, and others) require materials with high sensitivity to magnetic fields and with a $T_C$ close to 300 K. The formal charge state of manganese plays a key role in determining the Curie temperature of manganites: increasing the fraction of $Mn^{4+}$ from 15 to 40% (relative to the total Mn content) raises $T_C$ from 180 to 360 K [2]. The valence state of Mn can be controlled by varying oxygen stoichiometry or by heterovalent cation substitutions. $La_{1-x}M^{2+}_xMnO_3$ solid solutions with $M^{2+}$ = alkaline-earth metal have been studied most extensively [4–7]. It is of interest to substitute alkali-metal ions for La because the large difference in valence may lead to changes in structure and magnetic properties. Given that La and Na are close in ionic radius ($R_{La^{3+}} = 1.36$ Å, $R_{Na^+} = 1.39$ Å) [8], the $La_{1-x}Na_xMnO_{3\pm\gamma}$ solid-solution system is of considerable interest.

The studies of $La_{1-x}Na_xMnO_{3\pm\gamma}$ solid solutions in [9, 10] were limited to $x = 0.10$ and $x = 0.10$ and 0.30, respectively. According to Perekalina *et al.* [10], the $T_C$ of ceramic samples depends on the heat-treatment temperature. There is no agreement among different groups as to the optimum heat-treatment conditions in the solid-solution system under consideration: the reported solid-state sintering temperatures range from 1290 [11] to 1470 K [12–14]. Because of the appreciable Na volatility at high temperatures, the reported composition ranges of the $La_{1-x}Na_xMnO_{3\pm\gamma}$ solid solution also differ significantly: $x \le 0.2$ [15], $x \le 0.25$ [11], and $x \le 0.30$ [10, 12, 13]. Sintering samples embedded in Na-enriched manganite powder, Ganin [14] was able to raise the Na content of the solid solution to $x = 0.40$.

In most works [10–15], $La_{1-x}Na_xMnO_{3\pm\gamma}$ solid solutions were reported to crystallize in the rhombohedral space group $R\bar{3}c$. At the same time, there were reports that the rhombohedral distortion takes place for $x \ge 0.15$ in $Nd_{1-x}Na_xMnO_3$ [16] and $x > 0.065$ in $La_{1-x}Na_xMnO_{3\pm\gamma}$ [17] and that, at lower Na contents, doped lanthanum manganite has an orthorhombic structure. As pointed out in [18], the presence of lanthanum and oxygen vacancies leads to the formation of an $R\bar{3}c$ structure with a high magnetoresistance and $T_C$, while manganese vacancies result in a *Pbnm* orthor-

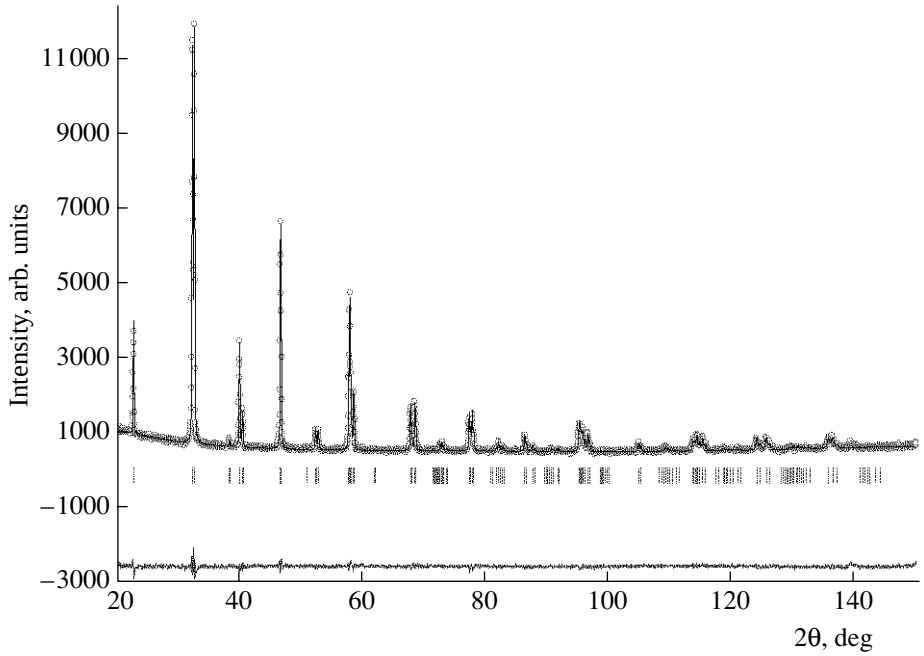


**Fig. 1.** Observed (points) and calculated (solid line) XRD patterns of the $La_{0.92}Na_{0.058}\square_{0.022}MnO_{3.068}$ ceramic prepared at 1420 K.

hombic structure and semiconducting behavior of resistivity. According to Shimura *et al.* [15], the decrease in the positive charge of the lanthanum sublattice upon Na substitution causes no changes in the valence state of Mn but increases the occupancy on the Mn site. Note that, in most works dealing with $La_{1-x}Na_xMnO_{3\pm\gamma}$, no

**Table 1.** Na content of polycrystalline $La_{1-x}Na_xMnO_{3\pm\gamma}$ samples sintered at 1420 K

| wt % Na | | $x$ | | $\Delta x$ ($x_{nominal} - x_{assay}$) | $\Delta x/x_{nominal}$ |
|---|---|---|---|---|---|
| nominal | assay | nominal | assay | | |
| 0.795 | 0.580 | 0.080 | 0.058(4) | 0.0216 | 0.27 |
| 0.982 | 0.751 | 0.100 | 0.076(0) | 0.0240 | 0.24 |
| 1.221 | 0.928 | 0.120 | 0.091(2) | 0.0288 | 0.24 |
| 1.441 | 1.111 | 0.140 | 0.108(0) | 0.032 | 0.23 |
| 1.667 | 1.260 | 0.160 | 0.121(0) | 0.039 | 0.24 |

**Table 2.** Formal charge state of Mn and oxygen nonstoichiometry γ in $La_{1-x}Na_xMnO_{3\pm\gamma}$ solid solutions sintered at 1420 K

| Actual composition | $Mn_{total}$, % | $Mn^{3+}$, % | $Mn^{4+}$, % | Formal charge on Mn | γ |
|---|---|---|---|---|---|
| $La_{0.92}Na_{0.058}\square_{0.022}MnO_{3.068}$ | 23.6 | 16.1 | 7.5 | 3.32 | 0.068 |
| $La_{0.90}Na_{0.076}\square_{0.024}MnO_{3.043}$ | 23.9 | 16.5 | 7.4 | 3.31 | 0.043 |
| $La_{0.88}Na_{0.091}\square_{0.029}MnO_{3.016}$ | 24.2 | 16.9 | 7.3 | 3.32 | 0.016 |
| $La_{0.86}Na_{0.108}\square_{0.032}MnO_{2.994}$ | 24.4 | 17.1 | 7.3 | 3.33 | –0.006 |
| $La_{0.84}Na_{0.121}\square_{0.039}MnO_{2.973}$ | 24.6 | 17.7 | 7.6 | 3.31 | –0.027 |

Note: □ designates an La vacancy.

**Table 3.** Crystallographic data for $La_{1-x-y}Na_x\square_yMnO_{3\pm\gamma}$ samples sintered at 1420 K

| $x$ | 0.058 | 0.076 | 0.091 | 0.108 | 0.121 |
|---|---|---|---|---|---|
| Lattice parameters | | | | | |
| $a$, Å | 5.5206(2) | 5.5190(3) | 5.5157(2) | 5.5102(2) | 5.5084(4) |
| $c$, Å | 13.3416(3) | 13.3414(4) | 13.3436(3) | 13.3400(3) | 13.3393(6) |
| $V$, Å$^3$ | 352.13(2) | 351.93(3) | 351.56(2) | 350.77(2) | 350.52(4) |
| $c/a$ | 2.4167 | 2.4174 | 2.4192 | 2.4210 | 2.4216 |
| Positional parameter of O | | | | | |
| $x/a$ | 0.456(2) | 0.454(3) | 0.452(2) | 0.454(2) | 0.445(2) |
| Bond distance, Å | | | | | |
| Mn–O | 1.959(1) | 1.960(2) | 1.961(1) | 1.958(1) | 1.960(2) |
| Thermal parameters | | | | | |
| La | 0.89(3) | 0.10(7) | 0.31(3) | 0.44(3) | 0.47(6) |
| Na | 0.89(3) | 0.10(7) | 0.31(3) | 0.44(3) | 0.47(6) |
| Mn | 0.26(5) | 0.2(1) | 0.31(4) | 0.27(4) | 0.26(9) |
| O | 2.7(3) | 1.1(6) | 2.0(3) | 2.0(3) | 0.3(6) |
| Site occupancies | | | | | |
| La | 0.920 | 0.900 | 0.880 | 0.860 | 0.840 |
| Na | 0.068 | 0.076 | 0.091 | 0.108 | 0.121 |
| Mn | 1.000 | 1.000 | 1.000 | 1.000 | 1.000 |
| O | 3.10(6) | 3.1(1) | 3.15(6) | 3.09(5) | 3.1(1) |
| Formal charge on Mn | 3.4(1) | 3.4(2) | 3.5(1) | 3.5(1) | 3.5(2) |
| Divergence factors | | | | | |
| $R_b$, % | 5.28 | 3.96 | 5.53 | 5.38 | 6.85 |
| $R_f$, % | 7.58 | 4.62 | 7.09 | 7.30 | 7.88 |

Note: Space group $R\bar{3}c$: La in 6*a* (0 0 1/4), Mn in 6*b* (0 0 0), and O in 18*e* (*x* 0 1/4).

data were reported on the magnetoresistive response of these materials, a characteristic essential for their practical application.

In this paper, we describe the structural, electrical, magnetic, and magnetoresistive properties of $La_{1-x}Na_xMnO_{3\pm\gamma}$ solid solutions in the composition range where ferromagnetic ordering may be achieved near room temperature.

## EXPERIMENTAL

Samples for this investigation were prepared by solid-state reactions, using appropriate mixtures of reagent-grade $NaCO_3$ and extrapure-grade $La_2O_3$ and $Mn_2O_3$ predried at 1120, 920, and 520 K, respectively. The starting mixtures were homogenized by vibration milling for 6–8 h in distilled water with corundum grinding media. Next, the mixtures were dried at 380–400 K, passed through a nylon 6 sieve, fired at 1170 K for 4 h, and then again homogenized by wet grinding. After addition of an aqueous solution of polyvinyl alcohol as a binder, the powder was pressed into disks 10 mm in diameter and 3–4 mm in thickness, which were then sintered at 1420–1500 K for 2 h.

Structural parameters of the resultant $La_{1-x}Na_xMnO_{3\pm\gamma}$ ceramics were determined by the Rietveld profile analysis method. X-ray diffraction (XRD) measurements were made on a DRON-4-07 powder diffractometer (Cu$K_\alpha$ radiation). XRD patterns were run in the angular range $2\theta = 10°$–$150°$ in a step-scan mode with a step size $\Delta 2\theta = 0.02°$ and a counting time of 10 s per data point. As external standards, we used $SiO_2$ ($2\theta$ calibration) and $Al_2O_3$ (NIST SRM1979 intensity standard). The $Mn^{3+}$ and $Mn^{4+}$ contents were determined by titration with an iodine thiosulfate solution. The iodine in the potassium iodide solution was

replaced by the chlorine resulting from the dissolution of a manganite sample in hydrochloric acid [19]. Na content was determined by flame spectroscopy using dissolved manganite samples.

The electrical resistivity of ceramic samples was measured by a four-probe technique from 77 to 370 K. The samples were rectangular in shape, $2 \times 3 \times 10$ mm in dimensions. Electrical contacts were made by firing silver paste. Magnetoresistance $(\rho_0 - \rho_H)/\rho_0$, where $\rho_0$ is the zero-field resistivity and $\rho_H$ is the resistivity in magnetic field $H$, was determined in applied fields of up to 1.2 MA/m.

## RESULTS AND DISCUSSION

We studied $La_{1-x}Na_xMnO_{3\pm\gamma}$ solid solutions with $x = 0.08$, 0.10, 0.12, 0.14, and 0.16. Chemical analysis of the $La_{1-x}Na_xMnO_{3\pm\gamma}$ samples sintered at 1420 K (Table 1) showed that the Na loss $\Delta x$ (and, accordingly, the amount of La vacancies) was proportional to $x$. The relative loss $\Delta x/x_{nominal}$ was 23–27%. The chemical analysis data for Mn in different valence states are presented in Table 2. It can be seen that the reduction in the positive charge of the lanthanum sublattice upon Na substitution causes no increase in the formal charge on Mn and is only possible owing to an increase in the amount of oxygen vacancies (decrease in $\gamma$), in accordance with earlier findings [15, 20, 21].

XRD examination showed that all of the synthesized materials were single-phase and had a rhombohedrally distorted perovskite structure. Figure 1 compares the observed and calculated XRD patterns for $x = 0.058$ ($x_{nominal} = 0.080$). The structural parameters (hexagonal setting) of the solid solutions are listed in Table 3. The Mn–O bond distance is seen to vary insignificantly with $x$, in accordance with chemical analysis data, which demonstrate that the valence state of Mn in $La_{1-x-y}Na_x\square_yMnO_{3\pm\gamma}$ is essentially independent of $x$.

The density of the ceramics increases linearly as the sintering temperature is raised to 1470 K (Fig. 2). Further increase in temperature leads to appreciable Na losses. Reducing the cooling rate was found to raise the density of the $La_{1-x-y}Na_x\square_yMnO_{3\pm\gamma}$ ceramics. In view of this, the samples were sintered at 1420–1470 K and then cooled at a rate below 200 K/h.

Figure 3 displays the temperature dependences of resistivity and magnetoresistance for $La_{1-x-y}Na_x\square_yMnO_{3\pm\gamma}$ ceramics. The $\rho(T)$ curves exhibit a maximum at a temperature $T_{max}$ that increases with $x$. Below $T_{max}$, the temperature coefficient of resistance is positive, $d\rho/dT > 0$ (metallic conduction), characteristic of ferromagnetic states. Above $T_{max}$, the conductivity is thermally activated ($d\rho/dT < 0$), typical of the paramagnetic state of doped manganites. The peak in magnetoresistance at $T_{max}$ is due to ferromagnetic ordering. The additional contribution to magnetoresistance at low temperatures may be associated with spin-dependent grain-boundary

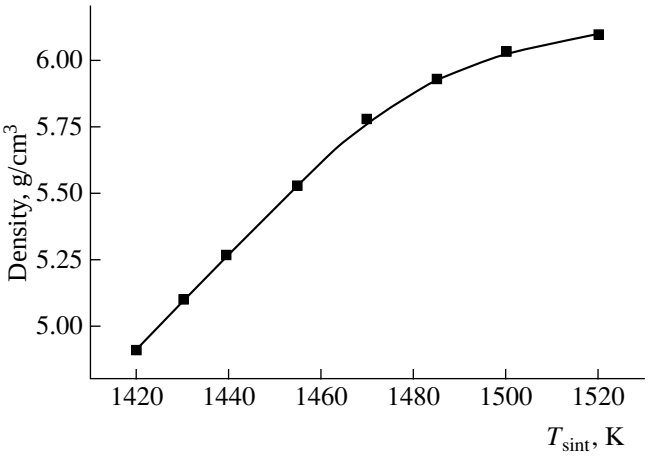


**Fig. 2.** Apparent density as a function of sintering temperature for ceramics of nominal composition $La_{0.88}Na_{0.12}MnO_{3\pm\gamma}$ (theoretical density, 6.48 g/cm$^3$).

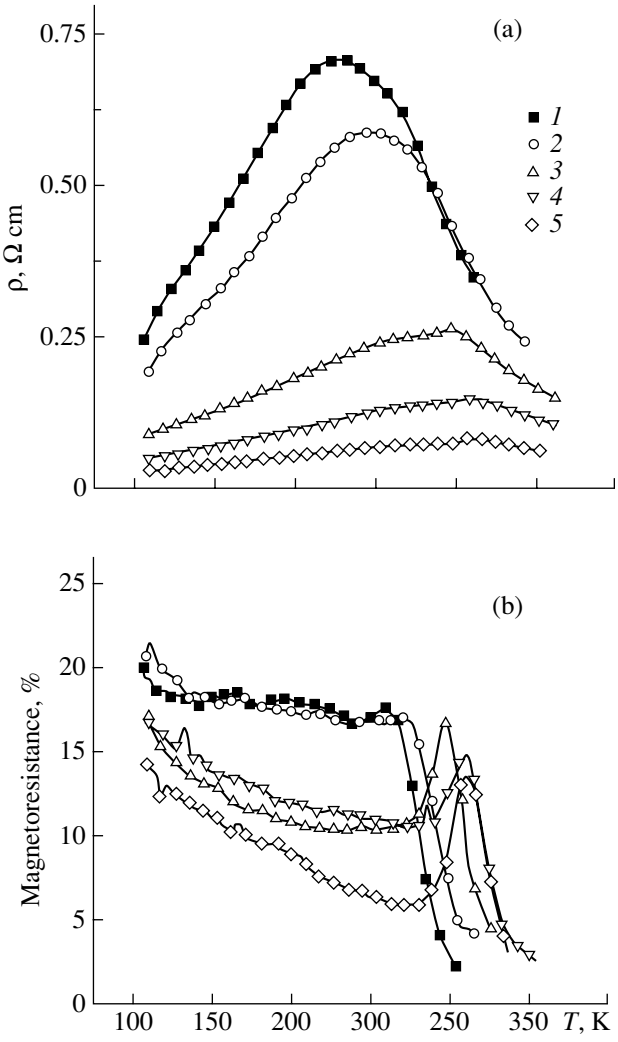


**Fig. 3.** Temperature dependences of (a) resistivity and (b) magnetoresistance for $La_{1-x-y}Na_x\square_yMnO_{3\pm\gamma}$ ceramics sintered at 1420 K: $x$ = (*1*) 0.0584, (*2*) 0.076, (*3*) 0.0912, (*4*) 0.108, (*5*) 0.121.

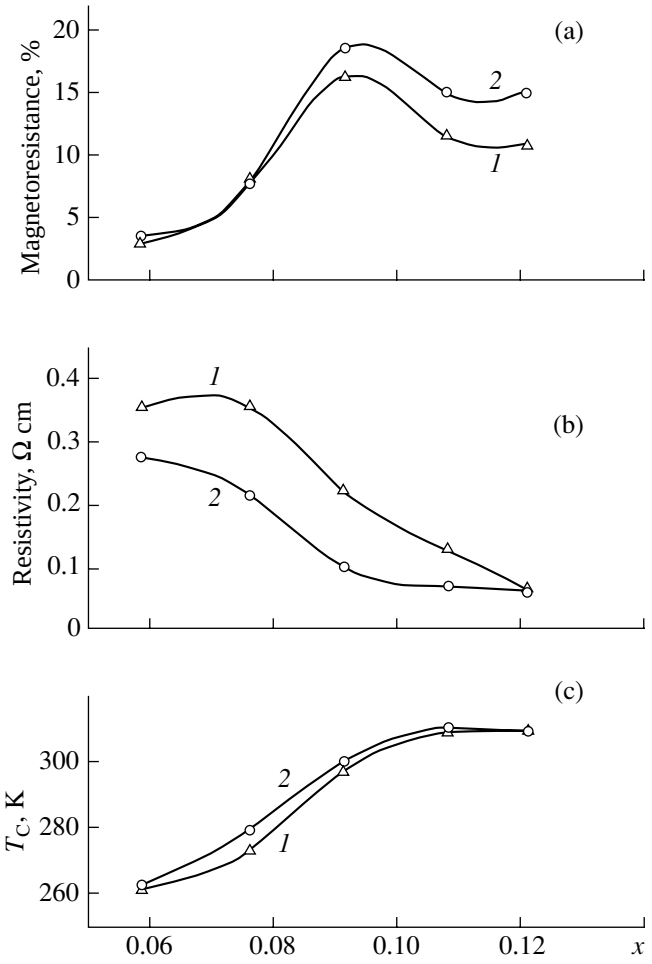


**Fig. 4.** Composition dependences of (a) magnetoresistance, (b) resistivity, and (c) $T_C$ for $La_{1-x-y}Na_x\square_yMnO_{3\pm\gamma}$ ceramics prepared by sintering at (*1*) 1420 and (*2*) 1440 K.

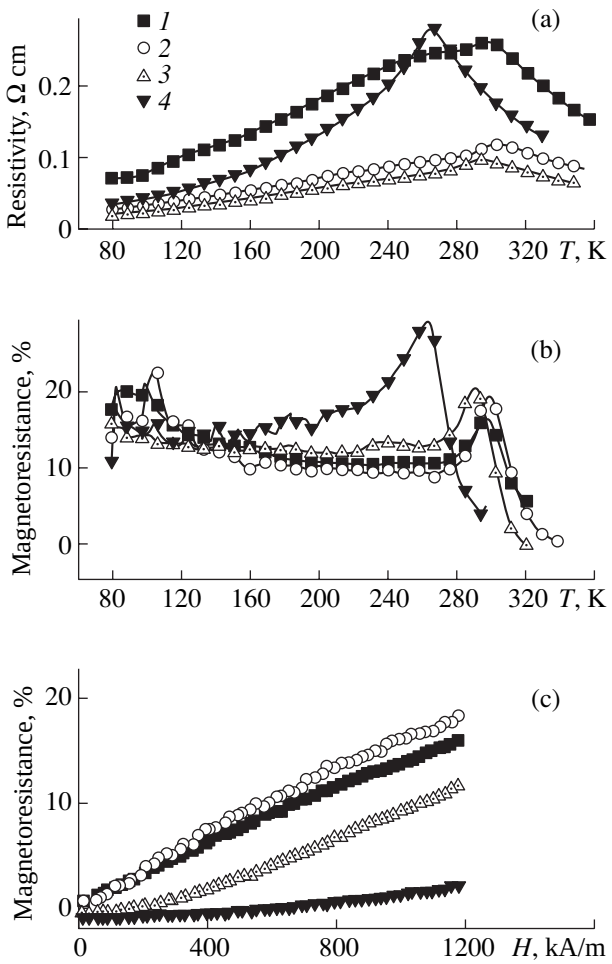


**Fig. 5.** (a) Resistivity and (b) magnetoresistance as functions of temperature and (c) 300-K magnetoresistance as a function of magnetic field for ceramics of nominal composition $La_{0.88}Na_{0.12}MnO_{3\pm\gamma}$ prepared by sintering at (*1*) 1420, (*2*) 1440, (*3*) 1470, and (*4*) 1520 K.

processes [22]. Since the Curie temperature usually coincides with the peak-magnetoresistance temperature, we determined $T_C$ as $T_{max}$ in the magnetoresistance versus $T$ curve.

The 300-K composition dependences of magnetoresistance and resistivity for $La_{1-x-y}Na_x\square_yMnO_{3\pm\gamma}$ are shown in Figs. 4a and 4b. Increasing the sintering temperature from 1420 to 1440 K reduces resistivity and increases magnetoresistance. The highest magnetoresistance (up to 20% at 300 K in a field of 1.2 MA/m) is observed in the composition range $x$ = 0.090–0.095 ($x_{nominal}$ = 0.12–0.13).

Although the formal charge state of Mn varies insignificantly, the Curie temperature of $La_{1-x-y}Na_x\square_yMnO_{3\pm\gamma}$ rises steadily as $x$ increases from 0 to 0.11 (Fig. 4c). $T_C$ depends not only on $x$ but also on $y$. The increase in $T_C$ with increasing sintering temperature at a given nominal composition is attributable to the increase in $y$ in $La_{1-x-y}Na_x\square_yMnO_{3\pm\gamma}$. It can be seen from Table 2 and Fig. 4c that $T_C$ grows at $y \le 0.032$ and $\gamma \ge 0$, whereas La and O vacancies reduce $T_C$. In particular, the maxima in the resistivity and magnetoresistance of the samples with the nominal composition $La_{0.88}Na_{0.12}MnO_{3\pm\gamma}$ sintered above 1440 K are shifted to lower temperatures (Figs. 5a, 5b).

Figure 5c illustrates the effect of magnetic field on the room-temperature magnetoresistance of the doped manganite. The magnetoresistance of the samples sintered at 1420–1440 K increases almost linearly with $H$ and attains 20%. At higher sintering temperatures, magnetoresistance varies nonlinearly. Note that the room-temperature magnetoresistance of bulk samples in other doped manganite systems is no higher than 8–15% in fields of up to 1.2 MA/m [23]. Given that the magnetoresistance of $La_{0.88}Na_{0.12}MnO_{3\pm\gamma}$ is an almost linear function of $H$, this material can be used as a sensitive element for magnetic-field measurements.

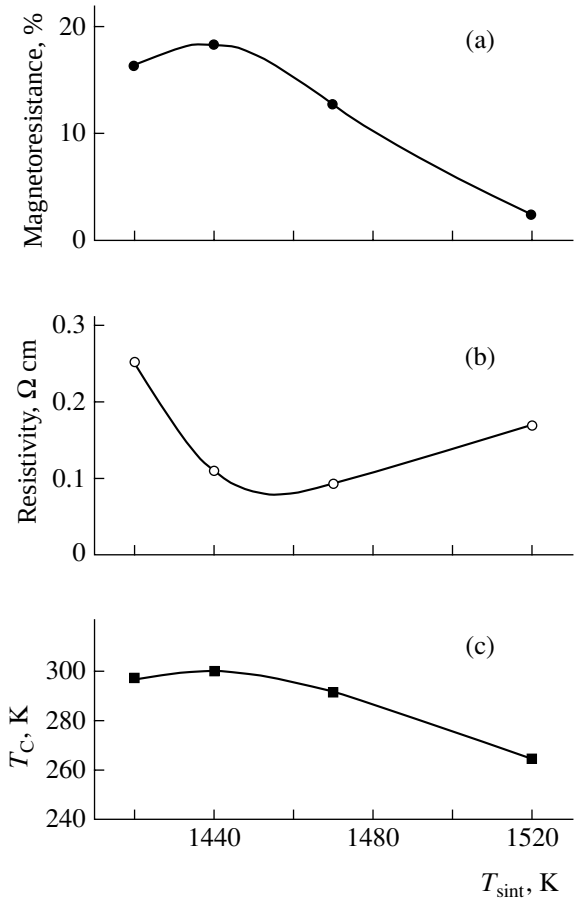


**Fig. 6.** (a) Magnetoresistance, (b) resistivity, and (c) Curie temperature as functions of sintering temperature for ceramics of nominal composition $La_{0.88}Na_{0.12}MnO_{3 \pm \gamma}$.

The $T_C$ and room-temperature resistivity and magnetoresistance versus sintering temperature data for the $La_{0.88}Na_{0.12}MnO_{3 \pm \gamma}$ ceramic (Fig. 6) indicate that the optimum sintering temperature is close to 1440 K.

## CONCLUSIONS

$La_{1-x}Na_xMnO_{3 \pm \gamma}$ solid solutions crystallize in the rhombohedral space group $R\bar{3}c$, which attests to the presence of La and O vacancies. The appreciable difference in valence between La and Na causes no changes in the valence state of Mn. At the same time, the ferromagnetic ordering temperature correlates with the Na content and the amounts of La and O vacancies. There are optimal deviations from stoichiometry ($y$ and $\gamma$) in $La_{1-x-y}Na_x\square_yMnO_{3 \pm \gamma}$ that ensure a $T_C$ close to room temperature and high magnetoresistance. The optimum sintering temperature of the solid solutions in air is determined. The synthesized materials are potentially attractive as room-temperature magnetic sensors with a magnetoresistance of up to 20% in a magnetic field of 1.2 MA/m.

## REFERENCES

1. Wollan, E.O. and Koehler, W.C., Neutron Diffraction Study of the Magnetic Properties of the Series of Perovskite-Type Compounds $[(1-x)La\,xCa]MnO_3$, *Phys. Rev.*, 1955, vol. 100, no. 2, pp. 545–548.
2. Nagaev, E.L., Lanthanum Manganites and Other Colossal Magnetoresistance Magnetic Conductors, *Usp. Fiz. Nauk*, 1996, vol. 166, no. 8, pp. 833–858.
3. Takura, Y., Uruchibara, A., Moritomo, Y., *et al.*, Giant Magnetotransport Phenomena in Filling Controlled Kondo Lattice System: $La_{1-x}Sr_xMnO_3$, *J. Phys. Soc. Jpn.*, 1994, vol. 63, no. 11, pp. 3931–3935.
4. Nowotny, J. and Rekas, M., Defect Chemistry of $(La,Sr)MnO_3$, *J. Am. Ceram. Soc.*, 1998, vol. 81, no. 1, pp. 67–80.
5. Cherepanov, V.A., Barkhatova, L.Yu., and Voronin, V.V., Phase Equilibria in the La–Sr–Mn–O System, *J. Solid State Chem.*, 1997, vol. 134, no. 1, pp. 38–40.
6. Takeda, Y., Nakai, S., Kojima, T., *et al.*, Phase Relation in the System $La_{1-x}A_xMnO_{3+z}$ (A = Sr and Ca), *Mater. Res. Bull.*, 1991, no. 2/3, vol. 26, pp. 153–162.
7. Lewis, R.A., Phonon Modes in CMR Manganites at Elevated Temperatures, *J. Supercond.*, 2001, vol. 14, no. 1, pp. 143–148.
8. Shannon, R.D., Revised Effective Ionic Radii and Systematic Studies of Interatomic Distances in Halides and Chalcogenides, *Acta Crystallogr., Sect. A: Cryst. Phys., Diffr., Theor. Gen. Crystallogr.*, 1976, vol. 32, no. 5, pp. 751–767.
9. Gubkin, M.K., Perekalina, T.M., Bykov, A.V., and Chubarenko, V.A., Electrical Conductivity of Some Perovskite Manganites, *Fiz.Tverd. Tela* (S.-Peterburg), 1993, vol. 35, no. 6, pp. 1443–1448.
10. Perekalina, T.M., Shapiro, L.Ya., Lipinski, I.E., and Cherkezyan, S.A., Electrical and Magnetic Properties of Na-doped Lanthanum Manganite, *Fiz. Tverd. Tela* (Leningrad), 1991, vol. 33, no. 3, pp. 681–684.
11. Troyanchuk, I.O., Mantytskaya, O.S., Shapovalova, E.F., and Pastushonok, S.N., Magnetic Properties of Lanthanum Manganite Doped with Li, Na, K, Tl, and Hg Ions, *Fiz. Met. Metalloved.*, 1997, vol. 83, no. 2, pp. 83–88.
12. Xu Heng-yi, Cao Qing-qi, Shen Ya-tao, and Zhang Shiyuan, Magnetoresistance of Manganate $La_{1-x}Na_xMnO_{3 \pm \gamma}$ at Room Temperature, *Nanjing Univ. Gongeng Caliliao*, 2001, vol. 32, no. 2, pp. 147–148.
13. Ye, S.L., Song, W.H., Wang, S.G., *et al.*, Large Room-Temperature Magnetoresistance and Phase Separation in $La_{1-x}Na_xMnO_3$ with $0.1 \le x \le 0.3$, *J. Appl. Phys.*, 2001, vol. 90, no. 6, pp. 2943–2948.
14. Ganin, A. Yu., Synthesis and Investigation of the $La_{1-x}Na_xMnO_{3+\delta}$ System, *Lomonosov Internet J.*, 2000, sect. 12, commun. 1151932 (http://www.nature.ru/db/msg.html?mid=1151932&s=120000000).
15. Shimura, T., Toshimura, H., Yoshiyiki, I., *et. al.*, Magnetic and Electrical Properties of $La_yA_xMn_wO_3$ (A = Na, K, Rb, and Sr) with Perovskite-Type Structure, *J. Solid State Chem.*, 1996, vol. 124, no. 2, p. 250.
16. Filonova, E.A., Zaitseva, N.A., and Petrov, A.N., Crystal Structure of Mixed Manganites $Nd_{1-x}M_xMnO_{3+\delta}$ (M =

Na, K, Ag; $0 \le x \le 1$), *Zh. Fiz. Khim.*, 2002, vol. 76, no. 2, pp. 278–283.

17. Bychkov, G.A., Pavlov, V.I., Bogush, A.K., and Kartashova, G.I., Abstracts of Papers, *XVIII Vsesoyuznaya konferentsiya po fizike magnitnykh yavlenii* (XVIII All-Union Conf. on the Physics of Magnetism), Kalinin, 1988, pp. 431–432.
18. Ran Niwas Singh, Shivakumara, C., Vacan Ihacharya, S., *et. al.*, Synthesis, Structure, and Properties of Sodium or Potassium-Doped Lanthanum Orthomanganites from NaCl or KCl Flux *J. Solid State Chem.*, 1998, vol. 157, no. 1, p. 19.
19. Borovskikh, L.V., Mazo, G.A., and Ivanov, V.M., Determination of the Mean Oxidation State of manganese in Mixed Manganites, *Vestn. Mosk. Univ., Ser. 2: Khim.*, 1999, vol. 40, no. 6, pp. 373–374.
20. Zouari, S., Ranno, L., and Cheikh-Rouhou, A., Effect of A Cation Size Variance on Structural and Physical Properties of Praseodymium Manganites $Pr_{0.85}(Na_{1-x}K_x)MnO_3$, *Solid State Commun.*, 2001, vol. 119, no. 8/9, pp. 517–521.
21. Boujelben, W., Cheikh-Rouhou, A., Ellouze, M., and Joubert, J.C., Vacancy Effect on Physical Properties in Lacunar $Pr_{0.7-x}\square_xBa_{0.3}MnO_3$ Oxides, *J. Magn. Magn. Mater.*, 2002, vols. 242–245, pp. 662–664.
22. Jin, S., Tiefel, T.H., McCormack, M., *et al.*, Thousandfold Change in Resistivity in Magnetoresistive La–Ca–Mn–O Films, *Science*, 1994, vol. 264, no. 5157, pp. 413–415.
23. Belous, A.G., V'yunov, O.I., Pashkova, E.V., *et al.*, Effects of Chemical Composition and Sintering Temperature on the Structure of $La_{1-x}Sr_xMnO_{3\pm\gamma}$ Solid Solutions, *Neorg. Mater.*, 2003, vol. 39, no. 2, pp. 212–222 [*Inorg. Mater.* (Engl. Transl.), vol. 39, no. 2, pp. 161–170].